Conductance of a plane containing random cuts

Jan Tobochnik
Department of Physics, Kalamazoo College, Kalamazoo, Michigan 49007

M. A. Dubson, M. L. Wilson, and M. F. Thorpe
Department of Physics and Astronomy and Center for Fundamental Materials Research, Michigan State University, East Lansing, Michigan 48824

(Received 15 June 1989)

In this paper we make the first careful comparison between a computer simulation and an experimental measurement of the conductance of a two-dimensional continuum random conducting medium. In the experiment horizontal and vertical slits are cut in a conducting sheet. The centers of the slits are randomly positioned, and the conductance is measured all the way to percolation. The measurements are consistent with the expected critical exponent for the conductance of $t=1.3$. The experimental results are compared with computer simulations of ants that are parachuted to random starting points and then diffuse with a Brownian motion. From the behavior at large times, the diffusion constant can be found and hence the conductance, using the Einstein relation. The agreement with experiment is good except near the critical point. We conclude that the analog experiment is superior to the digital computations in this continuum system. This is the reverse of the situation in discrete lattice systems.

I. INTRODUCTION

In the past decade there has been a great deal of attention given to the study of the conductance of random metal-insulator systems. Much of the work has involved computer simulations on discrete lattice systems. With the advent of efficient algorithms and large computers, such simulations can now be regarded as providing numerical solutions to any desired accuracy. Of particular interest has been the conductivity exponent t which is universal in two dimensions (2D) and given by $t=1.30\pm0.01$.[1] Analog experiments have also been performed on 2D lattice systems and the results are in good agreement with computer simulations.[2] However, much larger systems can now be handled by computer simulation and this is the preferred method. Analog experiments are also restricted to very simple geometries.

The situation is very different in continuum systems. The analog experiments are of about the same difficulty and quality as in discrete lattice systems. However, the digital simulations are very much more complex. The obvious way to proceed is via a finite-element algorithm that discretizes the system onto a finite mesh, making it formally similar to a lattice system. However, the drawback is that a prohibitively large number of points is required to reasonably describe even a simple inclusion, such as a circle. Thus for a given number of inclusions, orders of magnitude more points are needed than for the same number of inclusions in a lattice problem. Such calculations are still largely beyond the range of present day computers. Having said this, we should note that analog experiments can't be done in 3D and are restricted to simple geometries in 2D.

Recently a very simple alternative approach has been used by Schwartz and Banavar.[3] This involves an evaluation of the diffusion constant and hence the conductance via the Einstein relation. The diffusion constant is found by randomly parachuting ants onto a conducting medium containing insulating holes. If an ant lands on the medium, it is allowed to diffuse and at long times the diffusion constant is extracted using $\langle r^2\rangle=4Dt$, where the average is taken over many diffusing ants. We were interested to see just how good this technique could be in a tightly controlled situation. In particular, we wondered if this computer simulation for a continuum system could be superior to the corresponding analog experiment.

The layout of the paper is as follows. In Sec. II, we describe the experimental setup and the measurements. In Sec. III, we look at the initial slope of the conductance, which can be calculated exactly. In Sec. IV, we discuss the value of the critical density of cuts at percolation and in Sec. V we show that the measured conductivity exponent is consistent with $t=1.3$. In Sec. VI, we introduce two interpolation formulas, which give a good overall description of the conductance. In Sec. VII, we describe the diffusion algorithm and compare these results with the experiment. Finally we make some concluding remarks in Sec. VIII.

II. EXPERIMENTAL SETUP

Using a simple experimental technique described previously,[2] we have measured the dc electrical conductance of a 2D continuum percolation system. Using a computer-controlled digital x-y plotter, we cut a random pattern of horizontal and vertical slits in a sheet of aluminized Mylar. As the pattern is cut, a digital Ohm meter continuously monitors the resistance of the sheet, and the computer records the resistance as a function of the number of slits cut. The curve of conductance versus the number of slits is obtained in the time it takes for the plotter to draw a percolating pattern (about 8 h for a pattern of 15 000 slits).

The samples are aluminized Mylar sheets consisting of 0.005-in.-thick Mylar plastic covered with a 500-Å film of aluminum.[4] The sheet resistance of the film is about 1.9 $\Omega/\Box$ and varies by less than 1% over a 23×23-cm^2 sample. The sample resistance rises from 2Ω for an unscratched sheet to a few hundred ohms for patterns near the percolation threshold.

The slits are cut with a hot metallic finger, consisting of a small steel ball bearing embedded in the tip of an aluminum rod which contains a heating element. This hot tip is held by the pen holder of the plotter, and when it touches the sheet it sears the plastic, breaking the aluminum film on top. Proper adjustment of the current in the heating element results in reliable drawing of smooth continuous lines of uniform width. No buildup of material was ever observed on the ball-bearing tip, nor did it show evidence of wear throughout the experiment. We took great pains to ensure that the slits were continuous cuts, without any skipping or chatter. Drawing of "daisy-chain" patterns of slits allowed us to check thousands of slits for continuity and showed failure rates of less than 1 cut in 10 000. Further experimental details are given elsewhere.[2]

In Fig. 1 we show photographs of samples illustrating the pattern of cuts produced. The direction of external current flow is horizontal in both photographs. The photo on the left shows the results of a trial with horizontal cuts only. The photo on the right shows a random pattern of horizontal and vertical cuts. The sample is a square sheet with an edge length of 23.1 cm and the slit length is roughly 1/50 of that, producing, loosely speaking, a 50×50 continuum system. It is convenient to define the 23×23-cm^2 square as being a unit square, so that all lengths are measured in terms of this length scale. Actual lengths can be found by multiplying by 23 cm. The program that generates the pattern locates new cuts on a continuum with the centers randomly placed on the sample square with no underlying lattice structure. Slits are cut either horizontally or vertically with a probability of $\frac{1}{2}$. The cuts are thus freely interpenetrating. The underlying digital resolution of the plotter is 1 part in 5000 and is insignificant; it is less than the mechanical jitter in the placement of the pen.

We ran four trials of the horizontal-vertical patterns as well a trial with horizontal slits only and a trial with vertical slits only. Here and throughout this paper, hor-

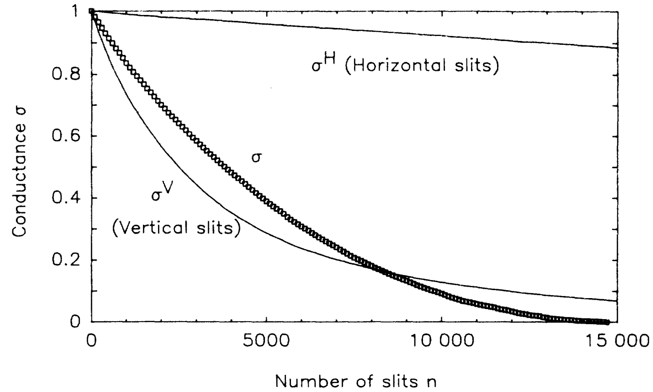

FIG. 2. Normalized conductance σ averaged over the four trials. The last data point corresponds to percolation as determined by the average over the four trials. Also shown are the results for σ^H and σ^V obtained with horizontal and vertical slits only for single trials.

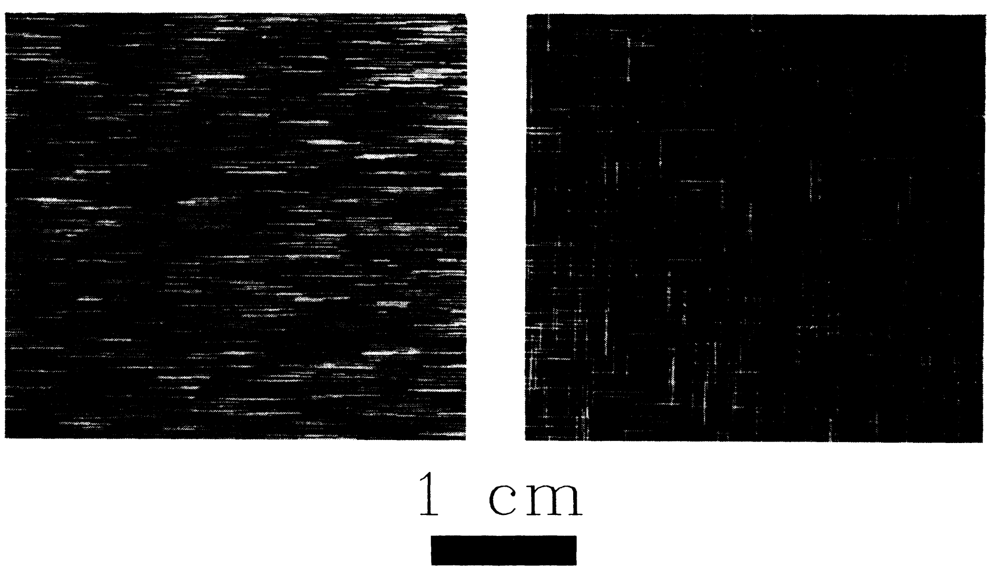

FIG. 1. Photo on the left shows a sample with only horizontal cuts. There are 35 000 cuts, which is far past the dilute limit of course. The photo on the right shows a random pattern of horizontal and vertical cuts at the percolation threshold. Each cut is approximately 4.5 mm long. Both photos show small pieces on the full samples.

izontal is the direction of external current flow. As explained in Sec. III, the trial with horizontal slits provides a measure of the effective aspect ratio of the slits, and the trial with vertical slits gives a check on the length of the slits.

Figure 2 shows the average conductance of the four trials as well as the results of the horizontal only and vertical only trials. Results of the four runs were quite consistent. The critical number of slits for percolation was $n_c = 14\,710 \pm 380$, with an uncertainty of one standard deviation for the four trials. The standard deviation of the mean is $380/\sqrt{4} = 190$.

III. INITIAL SLOPE

Comparison of these results with theory is complicated by the fact that the slits cut by the plotter are neither infinitesimally thin needles nor ellipses, rather, they are long, narrow bars. If, however, we assume that the slits are ellipses with high aspect ratio ($a/b \gg 1$), where a is the semimajor axis and b is the semiminor axis, then we can determine from the initial slopes of the conductance curves for the horizontal and vertical cases, shown in Fig. 2, both the length L of the slits and their aspect ratio a/b.

After these ellipses have been cut, the area fraction p of the conducting material remaining is given by

$$p = \exp(-\pi abn) , \tag{1}$$

where n is the area density of the insulating inclusions.[5,6] This formula is best understood as a power-series expansion

$$p = 1 - (\pi abn) + \tfrac{1}{2}(\pi abn)^2 - \tfrac{1}{6}(\pi abn)^3 + \cdots . \tag{2}$$

Here terms beyond πabn can be neglected when the density n is so low that overlaps between ellipses are rare. The term in $(\pi abn)^2$ corrects for the overlap of two ellipses, and the higher-order terms correct for the common area occupied by many ellipses.

The change in the conductance due to a single ellipse is a standard textbook problem.[7] If there are a few, widely separated parallel ellipses, the normalized conductances σ^H and σ^V for horizontal and vertical ellipses are given by [6]

$$\begin{aligned} \sigma^H &= 1 - (1-p)\frac{a+b}{a} , \\ \sigma^V &= 1 - (1-p)\frac{a+b}{b} . \end{aligned} \tag{3}$$

For small n, Eq. (2) gives $1-p = \pi abn$. Using this and $L = 2a$ for the lengths of the cuts, Eqs. (3) become

$$\sigma^H = 1 - \tfrac{1}{4} nL^2 \pi \frac{b}{a} \left[1 + \frac{b}{a} \right] = 1 - S^H n \tag{4}$$

and

$$\sigma^V = 1 - \tfrac{1}{4} nL^2 \pi \left[1 + \frac{b}{a} \right] = 1 - S^V n .$$

Our measurements of the initial slopes yield

$$S^H = (7.7 \pm 0.3) \times 10^{-6}, \quad S^V = (3.3 \pm 0.1) \times 10^{-4} . \tag{5}$$

From these measured slopes, Eqs. (4) yield

$$1/L = 49.3 \pm 0.7, \quad a/b = 42.9 \pm 2.1 . \tag{6}$$

Note that because the unit square is actually 23.1×23.1 cm^2 the size of the slits is $L = 2a = 4.69$ mm and the width $2b = 0.109$ mm.

To get an independent measure of the length L and the width w of the slits, the dimensions of several of the cuts were measured with a traveling microscope. The slits were found to have length 4.63 ± 0.15 mm and width 0.089 ± 0.008 mm. The uncertainties here represent variations from slit to slit rather than measurement errors. The sample edge length was found to be 23.08 ± 0.03 cm. These quantities can be expressed as

$$1/L = 49.9 \pm 1.6, \quad L/w = 52 \pm 4 , \tag{7}$$

which are close to the values obtained electrically in (6). This measured value of $1/L$ agrees with the value determined from the initial slope. The measured length/width ratio of the slits is roughly consistent with the a/b ratio inferred from the initial slope, although detailed comparison is difficult, since, as stated earlier, the slits are bar-shaped not elliptical. For the purposes of comparison with formulas for the conductance of random ellipse systems, we believe that the a/b value inferred from the electrical measurements is the more accurate and we will use this value later in analyzing the data.

The initial slope for the horizontal and vertical ellipse case can be found by averaging σ^H and σ^V in Eq. (4) to give

$$\sigma = 1 - \frac{1}{8} nL^2 \pi \left[1 + \frac{b}{a} \right]^2 = 1 - n/n_I ,$$

where, in the limit $a/b \ll 1$,

$$n_I L^2 = \frac{8}{\pi} \left[1 - \frac{2b}{a} \right] . \tag{8}$$

This expression gives a good fit to the data in Fig. 2 at small n and will be used later in Sec. VI.

IV. CRITICAL DENSITY

We now return to consider the measured critical slit number and its comparison with theoretical estimates. As stated above, the mean and standard deviation for our four trials was $n_c = 14\,710 \pm 380$. We may crudely estimate the expected spread in measured n_c's due to finite sample size as follows. We roughly estimate the correlation length by $\xi(n) = L[n_c/(n_c - n)]^{4/3}$, where L is the slit length.[8] Setting the correlation length equal to the sample size, $\xi = 1$, we have $\Delta n = n_c L^{-3/4}$. Taking $n_c = 14\,700$ and $1/L = 50$ yields $\Delta n = 780$. The measured spread in n_c is comparable to this crude estimate.

We define a dimensionless critical slit density by $\rho_c = n_c L^2$. Using the experimental values $n_c = 14\,710 \pm 190$ and $1/L = 49.9 \pm 1.6$, we have

$\rho_c = 5.9 \pm 0.4$. The dominant source of error here is the uncertainty in $1/L$.

Using numerical simulation, Xia and Thorpe[6] have estimated the critical concentrations for random ellipse systems. They find that their computer simulations are well fit by the formula

$$p_c = (1+4y)/(19+4y), \quad \text{where } y = b/a + a/b \ . \tag{9}$$

Inserting (9) into (1), we find that the critical concentration in the limit $b/a \ll 1$ is

$$\rho_c = n_c L^2 = \frac{18}{\pi}\left[1 - \frac{5b}{2a}\right] . \tag{10}$$

This expression yields, for the needle case (with $b/a = 0$), $\rho_c = 18/\pi = 5.73$ and, for the ellipse case (with $a/b = 42.9$), the value is depressed to $\rho_c = 5.40$. The measured value of $\rho_c = 5.9 \pm 0.4$ is somewhat higher than these predictions, but we emphasize that the expression (10) is not exact and was derived from numerical work on randomly oriented ellipses. Xia and Thorpe[6] also studied the case of horizontal and vertical ellipses, but less extensively. They concluded that p_c, and hence ρ_c, was the same for the random orientations as for the horizontal-vertical case to within their numerical accuracy.

V. CRITICAL EXPONENT

Sufficiently close to the percolation threshold, the conductance of a random metal-insulator composite is expected to show power-law behavior, $\sigma \sim (f_c - f)^t$, where f is the insulator fraction and t is the conductivity exponent. In 2D, $t \simeq 1.30$ in both lattice and continuum systems.[1,9]

Considerable caution must be exercised when attempting to extract a value for the conductivity exponent t from data on a small system such as ours. In Fig. 3 we have plotted the conductance curves of all four trials to display the scatter in the data. We have plotted conductance, not as a function of the number of slits n, but rather versus the fill fraction parameter $(f_c - f)/f_c$, where f is the effective fill fraction of the slits defined as

$$f(n) = 1 - \exp(-nA) \ . \tag{11}$$

Here A is an appropriate area of influence of a single slit, which we take to be the excluded area as defined by Balberg.[10] The excluded area of our slits of length $L = 1/50$ is $A = L^2/2 = 2 \times 10^{-4}$. The excluded area of an inclusion is the area within which the center of a second inclusion cannot be, if overlap is to be avoided. This is then averaged over all orientations; two in our case. The critical fill fraction $f_c = f(n_c)$ is taken to be the mean of our four trials, $f(n_c = 14\,710) = 0.95$. We have fit our data to a power law $\sigma \sim (f_c - f)^t$ over the fill fraction range between the two dashed vertical lines in Fig. 3. The vertical line on the left marks the composition at which the correlation length is half the sample size, $\xi = \frac{1}{2}$, where, as before, we estimate the correlation length with the expression $\xi = L[n_c/(n_c - n)]^{4/3}$. The vertical line on the right marks the composition at which

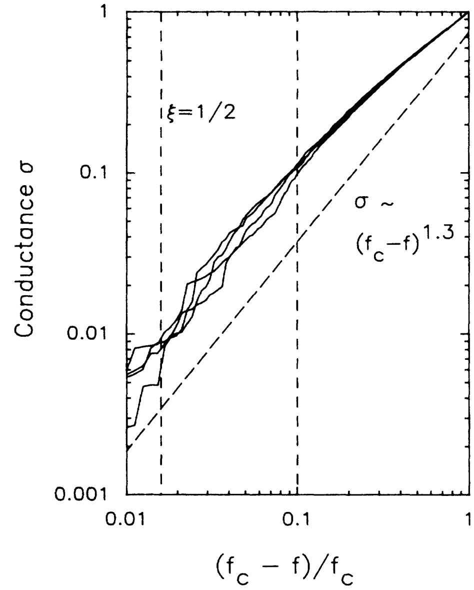

FIG. 3. Critical exponent t for the conductance is obtained from a log-log plot of the conductance versus fill fraction parameter $(f_c - f)/f_c$, where f is defined in the text. The vertical dashed lines indicate the region over which power-law behavior is observed. All four trials are shown individually, rather than averaged as in Fig. 2.

$(f_c - f)/f_c = 0.1$. This power-law window corresponds to $9570 < n < 13\,390$ or $0.09 < (n_c - n)/n_c < 0.35$. A nonlinear least-squares fit over this window yields $t = 1.30 \pm 0.03$, where the uncertainty reflects statistical uncertainty only and takes no account of possible systematic errors in our fitting procedure. We emphasize that the value for t obtained by this kind of power-law fit is quite sensitive to the assumed form of the power law. For instance, a fit of our data to $G \sim (n_c - n)^t$ (using n as the composition parameter rather than f) yields $t \simeq 1.9$. We conclude that our data are consistent with a conductance exponent of $t = 1.30$ but the close agreement is fortuitous.

VI. INTERPOLATION FORMULAS

We can compare the experimental data with two approximate interpolation formulas for $\sigma = \sigma(n)$. These interpolation formulas are smooth, monotonic functions of n which incorporate all known information about the form of the function. The initial slope is known exactly, via n_I in (8); the percolation concentration n_c is known approximately in (10); and the conductivity exponent $t = 1.30$ is known from numerical studies and is believed to be universal in 2D. The first formula was given by Xia and Thorpe:[6]

$$\sigma = \left[1 - \frac{n}{tn_I} - \frac{n^2(tn_I - n_c)}{tn_I n_c^2}\right]^t ,$$

which we refer to as formula A. A second form can be written

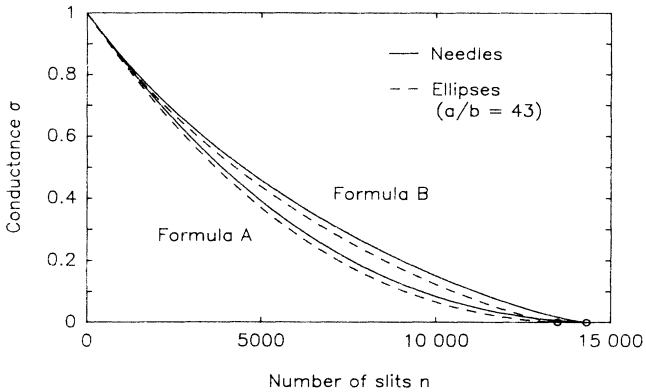

FIG. 4. Two interpolation formulas (A) and (B) are shown in the needle limits and for aspect ratios $a/b=43$. The circles indicate the percolation point for needles and ellipses.

$$\sigma=\left[\left(1-\frac{n^2}{n_c^2}\right)\Big/\left(1+\frac{n}{tn_I}\right)\right]^t .$$

which we refer to as formula B. These two expressions are not unique, of course, nor is there any *a priori* reason to prefer one over the other.

The values of n_c and n_I depend on the aspect ratio a/b in Eqs. (8) and (10). In Fig. 4, we show the sensitivity of the conductance to a/b by plotting formulas A and B for the needle case ($a/b=\infty$) and for the case $a/b=43$, which corresponds to our experiment. We use $L=1/50$ from which Eq. (10) gives $n_c=14\,320$ (needles) and $n_c=13\,490(a/b=43)$. Note that the experimentally determined $n_c=14\,710\pm380$ when averaged over the four samples.

In Fig. 5, we compare the experimental data with the two formulas, again using Eqs. (8) and (10) for n_I and n_c with $a/b=43$ and $L=1/50$. Both interpolation formulas have the same slope, given by n_I in Eq. (8), at small n, which agrees well with the experimental results. Indeed, for small n, $\sigma=(\sigma^H+\sigma^V)/2$, as can be seen from Fig. 2. The data lie generally between the two curves but some-

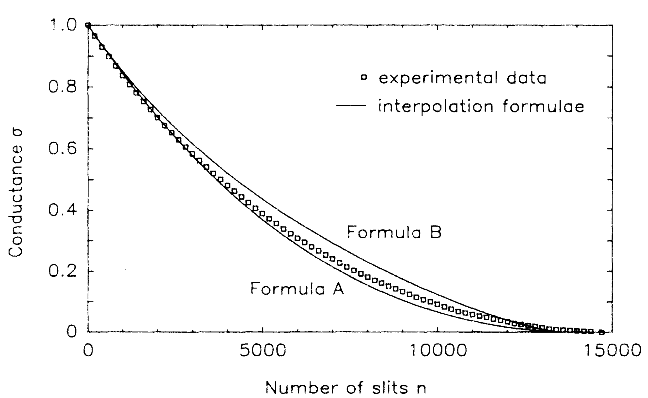

FIG. 5. Experimental data from Fig. 2 is shown plotted against the two interpolation formulas (A) and (B) with the aspect ratio $a/b=43$ and $L=1/50$.

what closer to formula A. If, instead of using Eq. (10) for n_c, we use the experimentally determined value of $n_c=14\,710$ (thereby forcing a fit at n_c), then the data lie even closer to formula A.

VII. DIFFUSION COMPUTATIONS

The probability $P(\mathbf{r},t)$ of a random walker (ant) being at position $\mathbf{r}$ at time t is governed by the diffusion equation[11]

$$D\nabla^2P(\mathbf{r},t)=\partial P(\mathbf{r},t)/\partial t \tag{12}$$

in a medium characterized by a position-independent diffusion constant D. If the ant is initially at the origin, then the solution to (12) is given by

$$P(\mathbf{r},t)=(\pi Dt)^{-1}\exp[-r^2/(4Dt)] , \tag{13}$$

from which we can calculate the second moment

$$\langle r^2\rangle=4Dt . \tag{14}$$

In order to apply these results to an inhomogeneous system, the diffusion process must take place over sufficiently long times that the behavior can be described by an effective diffusion constant. During this time the ant traverses lengths greater than the correlation length. Thus (14) is only expected to hold at long times. A more detailed critique of this method will be given in a subsequent publication.[12] In the present work, we use a pragmatic approach and let the ant diffuse for long enough times that linear behavior is obtained. This method has been successfully exploited on lattices,[13] but is just recently being applied to the continuum case. The conductance σ is obtained from the diffusion constant D via the Einstein relation[14]

$$\sigma=n_e e^2 D/(k_B T) , \tag{15}$$

where n_e is the number of carriers with charge e per unit area, and T is the temperature. We envisage the diffusing ants to be independent, so that the density n_e is not important and can be eliminated if we write

$$\sigma=D/D_0 , \tag{16}$$

where the subscript zero refers to the case where no needles are present and the conductance of the sheet without cuts is unity. The actual value of the charge e of the diffusing carriers and the temperature T is irrelevant when we use (16), as we will do in what follows.

The simulation was performed in the following way. We first randomly place n needles in a square box. Then we parachute an ant at random into this box. In the case of needle inclusions it is impossible for the ant position to overlap a needle since the needles have no width. We then attempt to move the ant a fixed distance in one of four directions up, down, left, or right. Next we must decide if this move crosses a needle. If it does, then the move is rejected and time is incremented; otherwise, it is accepted. This procedure is known as the "blind ant" boundary algorithm.[15] Since the needles are aligned either parallel or perpendicular to the steps taken by the ant, we need only check those needles that are perpendicular to the last step. This cuts the CPU time for the simulation almost in half. To determine if an ant has moved through a needle, we use the following simple test. If the ant is moving up or down and the needle lies left to right, then the condition for crossing the needle is that the y coordinate of the ant minus the y coordinate of the needle changes sign as the ant moves and the x coordinate of the ant is between the x coordinates of the end points of the needle. A similar computation is done when the ant moves left or right. The needle end point coordinates, as well as needle type (parallel or perpendicular to the horizontal axis), are stored, so that these quantities do not have to be computed for each test. We then computed r^2 versus the time, and fitted to a straight line as shown in Fig. 6. The conductance σ is extracted from this straight line using

$$\langle (r/s)^2 \rangle = \sigma N_T , \tag{17}$$

where N_T is the number of time steps and s is the step size chosen to be $L/40$. The slope of the fitted line gives $\sigma = D/D_0$. For short times, the data include ants that are trapped in closed regions which would not contribute to the conductance. Thus we want the slope in the limit of long time. We choose to use only the data for the last 75% of each walk and find that within the statistical uncertainties of the simulation we do not see any deviation from linearity. Figure 6 shows an example of the data with some initial curvature and linear behavior after that.

The system size was always $25L \times 25L$, which was large enough that no ants would wrap around the system more than once. The system was broken up into small cells of size $L/2 \times L/2$ so that if the ant was in one cell, only the rather small number of needles in that cell and the appropriate neighboring cells needed to be checked. For n/n_c varying from 0.1 to 1.1 the mean number of needles in each cell varied from about 0.14 to 1.6. Here we take $n_c L^2 = 18/\pi$ to be given by Eq. (10) with $b/a = 0$. Periodic boundary conditions were used. Almost all of our results are based on averages over 1000 ants, each with a new needle configuration. Each ant attempted $N_T = 160\,000$ steps, so that if there were no needles we would expect $\langle (r/L)^2 \rangle$ to be 100. In our simulations the ants will move a much smaller distance due to the needle inclusions and thus it is unlikely that an ant will move a distance in any direction greater than $25L$, which is the maximum distance before wrapping around the system. With the above conditions, the acceptance rate for moves decreased very little, reaching 0.925 at $n/n_c = 1.1$. This suggests that our step size is certainly small enough to accurately sample the local geometry "seen" by the ant. The results of the simulation are shown in Fig. 7. They compare well with both the interpolation formulas and the experimental results, except near the critical density and at very low densities. At very low densities the inclusions are very far apart and thus the ants need to move much further to accurately sample this geometry, or the averages need to be taken over more ants. At the high densities the ants do not move very far, but it takes a long time before they effectively sample their local geometry. Thus at these high densities, we cannot sample the medium- and large-scale structures of the needle configurations without letting the ants move for a much longer time. There is some evidence by running the simulation at $n/n_c = 0.8$ twice as long, that the slope of $\langle r^2 \rangle$ decreases slightly. This is to be expected because results for the diffusion constant and hence conductance are only reliable if the diffusion time is so long that the ant samples length scales greater than the correlation length. In our simulation, the correlation length $\xi = L[n_c/(n_c - n)]^{4/3}$ exceeds the diffusion distance at $n/n_c = 0.7$. At that concentration, the ant diffuses a distance of about $5L$. In Fig. 7 we have indicated the condition $\xi > 5L$ at $n/n_c = 0.7$ beyond which we expect the results to become unreliable. For $n/n_c = 0.1$, the computations took about 18 h on a Sun 375 work station and about 54 h for $n/n_c = 1$. Much longer diffusion times would be needed to explore the critical region. The needle system is harder to deal with than other systems (such as disks), since near the critical

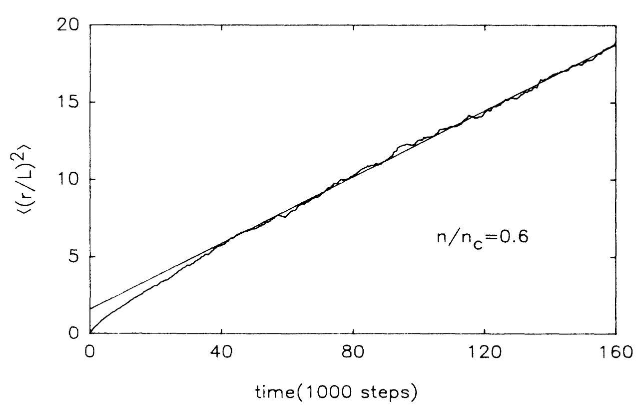

FIG. 6. Showing $\langle (r/L)^2 \rangle$ versus time t for $n/n_c = 0.6$ averaged over 1000 diffusing ants. here the step size $s = L/40$ and L is the length of the needle. Time is measured in units of 1000 steps. Thus the slope of the fitted line is the diffusion constant relative to the no needle system. Here the line was fitted to the data from time 40 to 160.

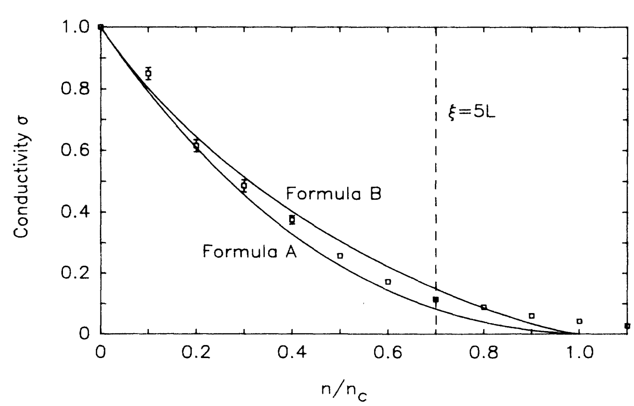

FIG. 7. Conductance σ obtained from the diffusing ant algorithm is compared to the two interpolation formulas (A) and (B) in the needle limit.

density, the density of needles is much greater than that of disks (thus increasing the mean CPU time per attempted step); yet there is still room to move around locally. Our conclusion is that for $n/n_c > 0.8$ we have not reached the asymptotic limit for $\langle r^2 \rangle$.

VIII. CONCLUSIONS

We have examined the conductances of sheets containing random cuts all the way up to the percolation concentration. Rather accurate results have been obtained in an analog experiment and these have been compared to results obtained from a digital simulation of an ant diffusing in the random medium. We were somewhat surprised to find that the results of the analog experiment were superior. This is in marked contrast to the similar situation in random lattice systems. Nevertheless, we regard the diffusing ant algorithm as clearly superior to finite-element methods. Looking ahead, it is unlikely that analog methods will improve much. In contrast, as better detailed algorithms and more computer power become available, we anticipate that the diffusing ant algorithm will eventually become the method of choice for the evaluation of transport coefficients in random continuum systems.

ACKNOWLEDGMENTS

We would like to thank J. R. Banavar and L. M. Schwartz for many valuable discussions. We should also like to thank M. DeVries for help with programming. This work was supported by the National Science Foundation under Grants No. DMR-8857364 and No. DMR-8714865. One of us (J. T.) acknowledges support from the Donors of the Petroleum Research Fund administered by the American Chemical Society and support from the Center for Fundamental Materials Research at Michigan State University for an extended visit to Michigan State University.

---

[1]D. J. Frank and C. J. Lobb, Phys. Rev. B **37**, 302 (1988).

[2]M. A. Dubson and J. C. Garland, Phys. Rev. B **32**, 7621 (1985).

[3]L. M. Schwartz and J. A. Banavar (unpublished); J. Tobochnik (unpublished).

[4]The material, called "mirrored Mylar," is sold by Ohio Graphics Arts, 26055 Every Road, Cleveland, OH 44120.

[5]A. S. Skal and B. I. Shklovskii, Fiz. Tekh. Polyprovdn. **7**, 1589 (1973) [Sov. Phys.—Semicond. **7** 1058 (1973)]; G. E. Pike and C. H. Seger, Phys. Rev. B **10**, 1421 (1974).

[6]W. Xia and M. F. Thorpe, Phys. Rev. A **38**, 2650 (1988).

[7]See, for example, L. D. Landau and E. M. Lifshitz, *Electrodynamics of Continuous Media* (Pergamon, Oxford, England, 1960) Chap. 2.

[8]This expression has the correct power-law behavior and approximately the correct amplitude. [J. P. Straley, in *Electrical Transport and Optical Properties of Inhomogeneous Media*, edited by J. C. Garland and D. B. Tanner (AIP, New York, 1978), p. 118].

[9]B. I. Halperin, S. Feng, and P. N. Sen, Phys. Rev. lett. **54**, 2391 (1985).

[10]I. Balberg, Phys. Rev. B **31**, 4053 (1985).

[11]S. Chandrasekhar, Rev. Mod. Phys. **15**, 1 (1943).

[12]M. DeVries, M. F. Thorpe, and J. Tobochnik (unpublished).

[13]See, for example, L. Puech and R. Rammal, J. Phys. C **35**, L1197 (1983); P. Argyrakis and R. Kopelman, Phys. Rev. B **29**, 511 (1984).

[14]V. K. S. Shante and S. Kirkpatrick, Adv. Phys. **20**, 325 (1971).

[15]P. G. de Gennes, La Recherche **7**, 919 (1976); D. Stauffer, *Introduction to Percolation Theory* (Taylor and Francis, London, 1985).